Proceedings of the ASME 2011 Internal Combustion Engine Division Fall Technical Conference
ICEF2011
October 2-5, 2011, Morgan Town, West Virginia, USA

ICEF2011-60141

EFFECT OF INLET AIR TEMPERATURE ON AUTO-IGNITION OF FUELS WITH DIFFERENT CETANE NUMBER AND VOLATILITY

Chandrasekharan Jayakumar
Wayne State University
Detroit, MI, USA.

Ziliang Zheng
Wayne State University
Detroit, MI, USA.

Umashankar M. Joshi
Wayne State University
Detroit, MI, USA.

Walter Bryzik
Wayne State University
Detroit, MI, USA.

Naeim A. Henein
Wayne State University
Detroit, MI, USA.

Eric Sattler
US Army Tank Automotive Research Development and Engineering Center
Detroit, MI, USA.

ABSTRACT

This paper investigates the effect of air inlet temperature on the auto-ignition of fuels that have different CN and volatility in a single cylinder diesel engine. The inlet air temperature is varied over a range of 30°C to 110°C. The fuels used are ultra-low-sulfur-diesel (ULSD), JP-8 (two blends with CN 44.1 & 31) and F-T SPK. Detailed analysis is made of the rate of heat release during the ignition delay period, to determine the effect of fuel volatility and CN on the auto-ignition process. A STAR-CD CFD model is applied to simulate the spray behavior and gain more insight into the processes that immediately follow the fuel injection including evaporation, start of exothermic reactions and the early stages of combustion. The mole fractions of different species are determined during the ignition delay period and their contribution in the auto-ignition process is examined. Arrhenius plots are developed to calculate the global activation energy for the auto-ignition reactions of these fuels. Correlations are developed for the ID and the mean air temperature and pressure.

INTRODUCTION

Concern about the depletion of petroleum reserves, rising prices of fuels, trade deficit and home land security enhanced the research on alternate fuels. Alternate fuels have different molecular structure than conventional fuels which affect auto-ignition and combustion in engines. In diesel engines, combustion is initiated by auto-ignition of the fuel-air mixture which is very sensitive to changes in the charge temperature. This paper investigates the effect of inlet air temperatures on auto-ignition and combustion of fuels with different properties especially cetane number (CN) and volatility. Sieber [1] conducted experiments in a constant volume vessel at different temperatures and concluded that the cetane number cannot provide a consistent and accurate measure of ignition quality of fuels whose ignition delay dependence on temperature and type of ignition process (single-stage or two-stage differ from those of the reference fuel blends of n-cetane and heptamethylnonane). Pickett [2] investigated the effect of fuel volatility and concluded that the volatility have an effect on ignition delay because it an important property that has an impact on the rate of fuel evaporation.

This investigation covered the following fuels: (a) ULSD (Ultra-low-sulfur-diesel), considered as the base fuel, (b) JP-8 which is the main military fuel [3, 4, 5] and (c) F-T SPK. Two blends of JP-8 were tested. One blend has a CN of 44 which is close to CN of ULSD and the other has a CN of 31 which is below the diesel specification limit in North America, but can be used in military vehicles. F-T SPK is a synthetic fuel made from a Gas-to-Liquids [3, 6] process known as Fischer-Tropsch conversion. F-T SPK has very low sulfur and aromatic contents and has very good auto-ignition characteristics [7]. A lubricity additive is added to F-T SPK before its use in the engine. The

Report Documentation Page

Form Approved
OMB No. 0704-0188

1. REPORT DATE	2. REPORT TYPE	3. DATES COVERED
01 OCT 2011	**Journal Article**	**01-10-2011 to 01-10-2011**

4. TITLE AND SUBTITLE
EFFECT OF INLET AIR TEMPERATURE ON AUTO-IGNITION OF FUELS WITH DIFFERENT CETANE NUMBER AND VOLATILITY

5a. CONTRACT NUMBER
5b. GRANT NUMBER
5c. PROGRAM ELEMENT NUMBER

6. AUTHOR(S)
Eric Sattler; Walter Bryzik; Chandrasekharan Jayakumar; Zilliang Zheng; Naeim Henein

5d. PROJECT NUMBER
5e. TASK NUMBER
5f. WORK UNIT NUMBER

7. PERFORMING ORGANIZATION NAME(S) AND ADDRESS(ES)
Wayne State University,471 West Palmer Avenue,Detroit,MI,48202

8. PERFORMING ORGANIZATION REPORT NUMBER
; #22033

9. SPONSORING/MONITORING AGENCY NAME(S) AND ADDRESS(ES)
U.S. Army TARDEC, 6501 E.11 Mile Rd, Warren, MI, 48397-5000

10. SPONSOR/MONITOR'S ACRONYM(S)
TARDEC

11. SPONSOR/MONITOR'S REPORT NUMBER(S)
#22033

12. DISTRIBUTION/AVAILABILITY STATEMENT
Approved for public release; distribution unlimited

13. SUPPLEMENTARY NOTES
Submitted to 2011 ASME INTERNAL COMBUSTION ENGINE DIVISION FALL TECHNICAL CONFERENCE ICEF 2011

14. ABSTRACT
This paper investigates the effect of air inlet temperature on the auto-ignition of fuels that have different CN and volatility in a single cylinder diesel engine. The inlet air temperature is varied over a range of 30?C to 110?C. The fuels used are ultra-low-sulfur-diesel (ULSD), JP-8 (two blends with CN 44.1 & 31) and F-T SPK. Detailed analysis is made of the rate of heat release during the ignition delay period, to determine the effect of fuel volatility and CN on the auto-ignition process. A STAR-CD CFD model is applied to simulate the spray behavior and gain more insight into the processes that immediately follow the fuel injection including evaporation, start of exothermic reactions and the early stages of combustion. The mole fractions of different species are determined during the ignition delay period and their contribution in the auto-ignition process is examined. Arrhenius plots are developed to calculate the global activation energy for the auto-ignition reactions of these fuels. Correlations are developed for the ID and the mean air temperature and pressure.

15. SUBJECT TERMS

16. SECURITY CLASSIFICATION OF:			17. LIMITATION OF ABSTRACT	18. NUMBER OF PAGES	19a. NAME OF RESPONSIBLE PERSON
a. REPORT	b. ABSTRACT	c. THIS PAGE			
unclassified	**unclassified**	**unclassified**	**Same as Report (SAR)**	**11**	

experimental results for the ignition delay are analyzed to calculate the global activation energy for the auto-ignition processes of each fuel. A STAR-CD CFD model is applied to gain a better understanding of the physical and chemical process that lead to auto-ignition and combustion.

EXPERIMENTAL SET-UP

Engine Set-up:

The engine is a small-bore, research type, high speed, 4-valve, single-cylinder direct-injection diesel engine, bore = 79.5 mm, stroke =85 mm and geometric C.R. = 20:1. The engine is equipped with a common rail injection system and a solenoid operated injector, with a 320 mini-sac, 6-hole nozzle (0.131 mm in diameter). Water, oil and fuel systems are run independent of the engine. The injection timing, pulse duration and rail pressure are controlled by an open ECU. A detailed description of the experimental set-up can be found in [8]. The test matrix and experimental conditions are given in Appendix A. Fuel properties are given in Appendix B.

SIMULATION MODEL AND ASSUMPTIONS

STAR-CD, an interactive CFD simulation software package coupled with chemical kinetics mechanisms (using DARS-CFD), is applied to simulate engine conditions [9]. Es-ice software is used to create the sector mesh of the combustion chamber. Pro-STAR is used to set other parameters like atomization, combustion model, injection parameters, time-step resolutions etc. Unlike many other CFD software which compress and expand the mesh based on piston motion, this software adds/removes cells in the mesh based on piston motion using mass, energy and species conservation laws.

The simulation is for engine operation under the following conditions: 3bar IMEP, 1500 rpm, 1.1 bar intake pressure, SOI: 2.2 CAD bTDC, EGR=0% and swirl ratio = 3.77. The model assumes a Lagrangian approach to define spray/droplet behavior. The software considers droplet trajectories, droplet break-up, collision and coalescence, wall interaction, wall heat transfer and droplet evaporation. Sector is defined by a cylindrical co-ordinate system. The sector mesh has 560,000 cells (70 x 50 x 160). Combustion mechanism currently being used in this software is for n-heptane and has 33 species and 122 reactions. The inputs used in the model are fuel, speed, swirl ratio, initial pressure and temperature, boundary conditions (wall, dome and piston crown) and time-step resolutions. The outputs are chamber temperature, pressure, density, species concentration, rate of heat release etc.

SIMULATION RESULTS AND DISCUSSIONS:

Simulation of the contribution of fuel evaporation in RHR

To determine the contribution of fuel evaporation in the negative RHR after the start of injection, a comparison is made between the model results for heptane evaporation in nitrogen and combustion in air. Fig. 1 shows both traces are the same from SOI at 2.2 CAD bTDC to 1.8 CAD bTDC, after which they start to separate, indicating the start of combustion chemical reactions. The point of separation is termed POI (Point Of Inflection) at which the exothermic combustion reactions start. The details of the exothermic reactions are explained in the next section of this paper. The trace for the RHR in the nitrogen atmosphere continues to drop at a slower rate until the EOI at 0.8 CAD aTDC, starts to rise again as the evaporation and heating the vapor continues and eventually joins the motoring trace.

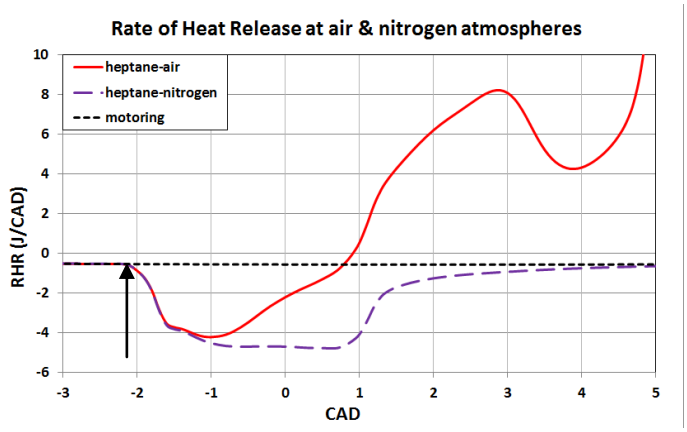

Figure 1: RHR for injection of heptane in air and nitrogen

Simulation of RHR produced from the auto-ignition and combustion reactions

Inlet air temperature 110°C

Figure 2 shows the mole fractions of different species at 110°C and the RHR from the start of fuel injection at 2.2 CAD bTDC to the end of ignition delay period at 110°C and 80°C. The mole fractions of 33 species are determined in the simulation model, but only the mole fractions of the intermediate species O, H, OH, HO_2, CH_2, C_2H_3, C_2H_5, C_3H_7 and HCHO will be presented in this paper to demonstrate their behavior and for the discussion of the results. The detected heat release due to the exothermic reactions starts at 1.8 CAD bTDC or 0.4 CAD (0.44 ms) after SOI. At 1.8 CAD bTDC all species, except HCHO, are produced at very low mole fractions. The mole fractions of the species increase at a sharp rate for 0.4 CAD, during which the RHR drops sharply and becomes negative. This is followed by an increase in the mole fractions of all the species, except HCHO, by one to three orders of magnitude. The rate of increase declines and the mole fractions reach a plateau after another one CAD. The formaldehyde (HCHO) behaves in a different way as it starts to appear after all the other species are close to their plateau. HCHO increases at an accelerating rate till it reaches its peak. It is noticed that the increase in HCHO is associated with relatively smaller changes in the mole fractions of H, O, OH and some hydrocarbon species. However, as HCHO reaches its peak at 3.5 CAD aTDC, most of the species

experience a dip for a period of one CAD. HCHO declines at a slow rate for two CADs, after which it declines sharply. Near the end of the slow decline of HCHO, species O, H and OH and some hydrocarbons increase sharply and reach a plateau after the decline in HCHO. Up to this point, the oxygen consumption and CO, H_2O formation is gradual and occurs at slow rates. CO_2 mole fraction is fairly small during this period. The sharp decline in HCHO is associated with sharp increases in H_2O and CO_2 and decline in O_2.

The bottom traces in Fig. 2 are for the RHR for inlet temperatures 110°C and 80°C and motoring. The trace for 80°C will be explained in the next section. The trace for 110°C is for the data explained in this section. As soon as injection starts at 2.2 CAD bTDC, the RHR becomes negative due to energy consumed in fuel evaporation as explained in the previous section. After 0.4 CAD, different species other than HCHO are produced at very low mole fractions. The sharp increase in these species is associated with a drop in RHR. RHR drops to a minimum at 1 CAD bTDC when the species are close to their plateau. RHR increases at a declining rate in the low temperature oxidation regime and reaches a maximum at 3 CAD aTDC. At 3 CAD aTDC HCHO is at its maximum rate of formation. The drop in RHR in the NTC regime takes one CAD where HCHO is close to its peak level and the other species are experiencing a dip in their level. The gradual drop in HCHO level up to 6 CAD aTDC is associated with a sharp increase in the level of most of the other species and RHR. Up to this point the increase in H_2O and CO is gradual but occurs at a slow rate, while CO_2 level is very low. After 6 CAD aTDC, HCHO concentration drops at a sharp rate; CO reaches close to its peak and H_2O and CO_2 concentrations increase at a high rate.

<u>Effect of lowering gas temperature on the auto-ignition of heptane</u>

The simulation is carried out at an inlet air temperature of 80°C and the results for the RHR are shown by the dotted-slashed line in the lower part of Fig 2. The drop in gas temperature produced the following effects: (a) Slowed down the oxidation reactions at the start of the low temperature combustion regime, (b) Increased RHR from the low temperature combustion regime, (c) Delayed the start of the NTC regime and (d) Increased the drop in RHR due to NTC regime.

At inlet temperatures, lower than 80°C, the model failed to produce auto-ignition, while the engine fired at temperatures lower than 80°C. The discrepancy between the model results and experiments is due to the fact that the fuel used in the experiments has molecules heavier and have better ignition qualities than heptane. However, the model for heptane has been helpful in pointing out to the role of some species such as HCHO in developing the NTC regime.

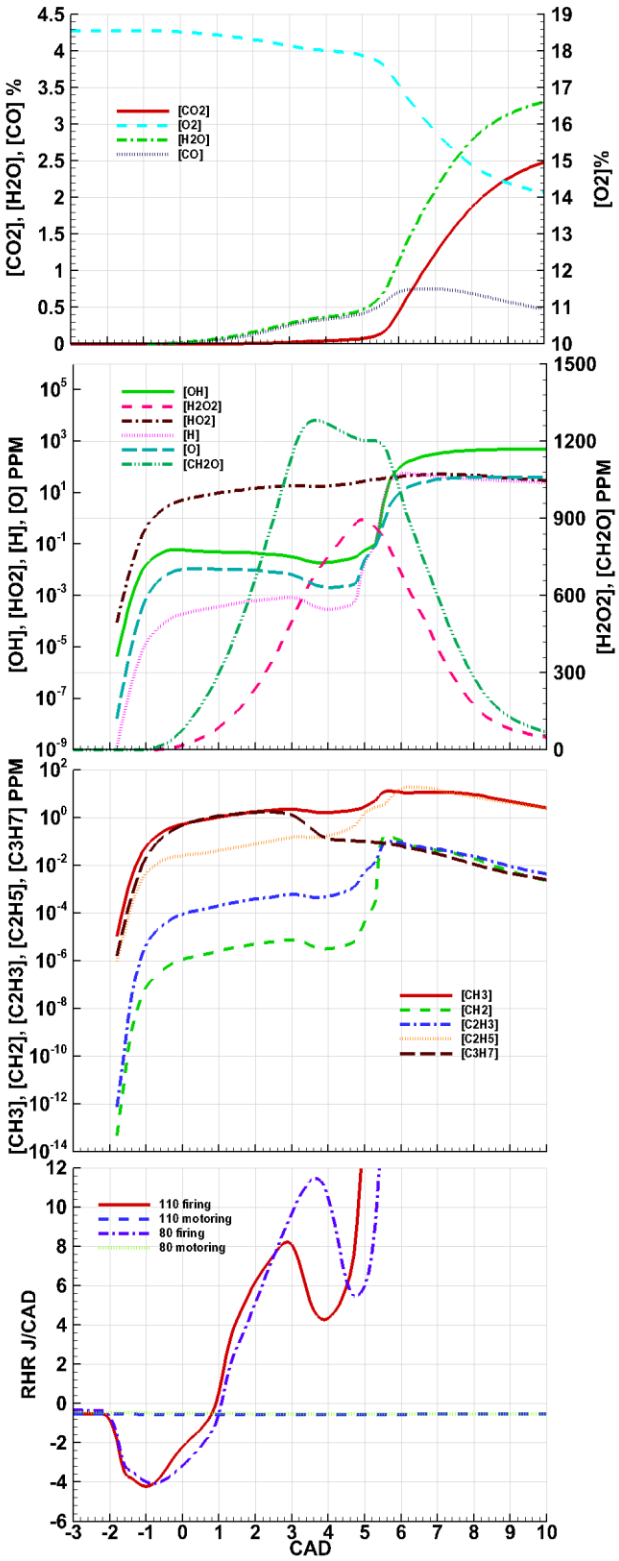

Figure 2: Mole fractions of different species at 110 C (top three figures) and Rate of heat release traces at 80°C &110°C intake temperatures (bottom figure).

EXPERIMENTAL RESULTS and DISCUSSONS

Comparison between the auto-ignition and combustion of fuels of different volatility and CN

This comparison is conducted at an engine speed of 1500 rpm and IMEP = 5 bar. The fuels tested are ULSD, JP-8 (44), JP-8 (31) and F-T SPK. Figure 3 shows RHR from the start of injection (SOI) at 2.5 CAD bTDC to 20 CAD aTDC for different fuels at 50°C intake temperature. F-T SPK has the shortest ID and the lowest peak of the RHR produced from the premixed combustion fraction. The low peak of RHR can be explained if we examine the combined effects of fuel volatility, CN, density and heating value (HV) on the RHR. High volatility enhances liquid evaporation [2] and the formation of an auto-ignitable mixture. High auto-ignition quality, expressed in terms of CN, accelerates the auto-ignition chemical reactions of the ignitable mixture and starts the combustion process which is considered to be the end the ID period. The fact that ID for F-T SPK is the shortest among all the fuels indicates that the CN number of the fuel, which is more than 29 higher than ULSD, has a strong impact on shortening the ID and limiting the premixed charge formation, in spite of the high volatility of F-T SPK. F-T SPK has the highest volatility (lowest flash point) among all the fuels. The flash point of F-T SPK is 37.8°C compared to 64°C for ULSD. Other factors that affect the RHR include density and HV. F-T SPK is the lightest fuel compared to ULSD. F-T SPK is 12% lighter than ULSD, but is 7% higher in heating value.

The situation is different if we compare between the peaks of RHR for JP-8 (44) and ULSD. The ID for JP-8 (44) which has 44 CN is shorter than ID for ULSD which has a higher CN of 45.3. In this case, the difference in volatility has more impact on the ID than CN. The flash point of JP-8 (44) is 56.8°C compared to 64°C for ULSD.

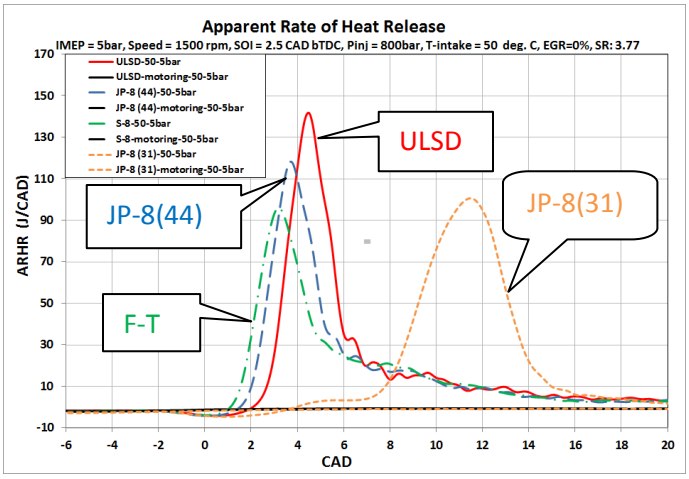

Figure 3: Rate of heat release for four fuels

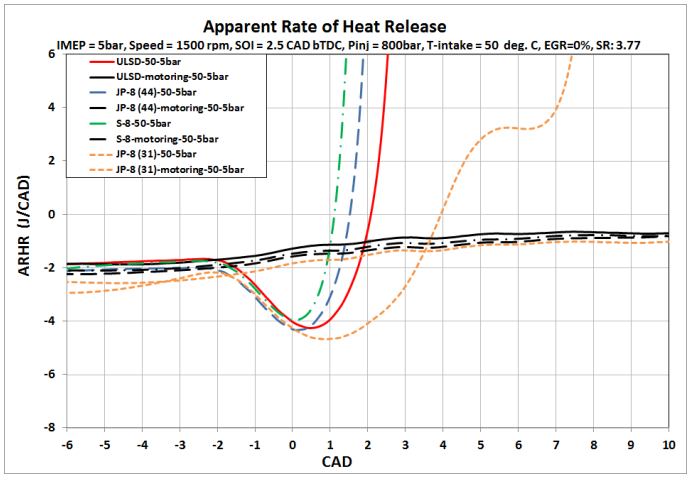

Figure 4: Details of RHR during auto-ignition and early stages of combustion

Figure 4 shows details of RHR during the ID and early stages of combustion and demonstrates the difference between the auto-ignition reactions of JP-8 (31) and the rest of the fuels. JP-8 (31) fuel experienced the low temperature combustion regime before the start of the high temperature combustion reactions. From literature it can be learned that other researchers have observed NTC behavior of fuels with investigations involving EGR [10, 11]. In this investigation, no EGR is used, yet JP-8 (31) exhibited NTC behavior. F-T SPK having the maximum cetane number demonstrated high rates of auto-ignition reactions crossing the motoring curve before all other fuels. JP-8 (44) demonstrated faster rates of auto-ignition reactions than ULSD despite have close cetane numbers due to its higher volatility. It is also reflected in their ignition delays shown in Arrhenius plots.

Effect of varying charge temperature on the auto-ignition of different fuels:

In this investigation, the charge temperature is varied by changing in the intake air temperature from 30°C to 110°C and the load from 3 bar to 5 bar IMEP. The results showed a drop in ID of all the fuels at higher charge temperatures. Also, the shapes of the RHR traces for all the fuels followed the shapes given in Fig. 3 and Fig.4 except for JP-8 (31).

Fig. 5 shows the ignition delays of different fuels at both loads with respect to the intake temperature. It can be observed that F-T SPK produced the shortest ignition delay compared to other fuels and JP-8 (31) produced the longest because of their highest and lowest cetane numbers, respectively. As discussed earlier JP-8 had a shorter ignition delay than ULSD because of its higher volatility, which enhances the rate of evaporation [2]. ULSD, JP-8 (44) and F-T SPK showed longer ignition delays at the higher load but JP-8 (31) showed a mixed trend.

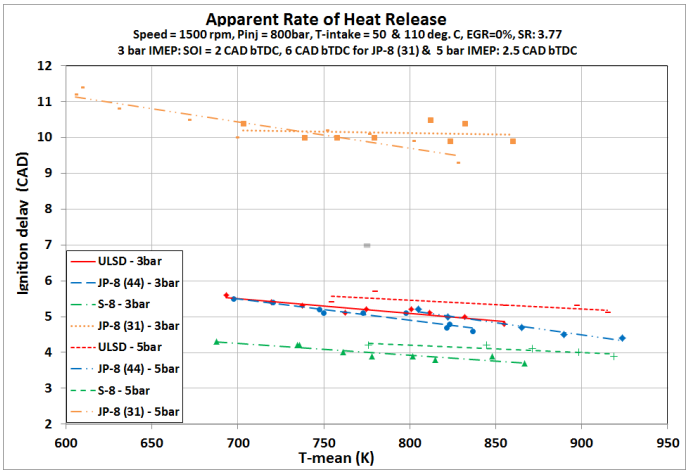

(Figure 5: Ignition delay vs mean temperature during ignition delay for different fuels at 3 bar and 5 bar IMEP respectively)

Effect of the charge temperature on auto-ignition and combustion of the JP-8 (31) fuel:

Figure 6 shows the RHR for the low cetane JP-8 at intake temperatures of 50°C and 110°C and IMEP = 3 bar and 5 bar. SOI is at 2.5 bTDC for 5 bar IMEP. At 3 bar IMEP, the engine misfired at SOI of 2 CAD bTDC which is set for the other fuels. For this, the injection timing is advanced to 6 CAD bTDC when the engine started to fire. The 60 degree increase (from 50°C to 110°C) in inlet temperature produced an increase in the gas temperature at SOI from 653K to 863K.

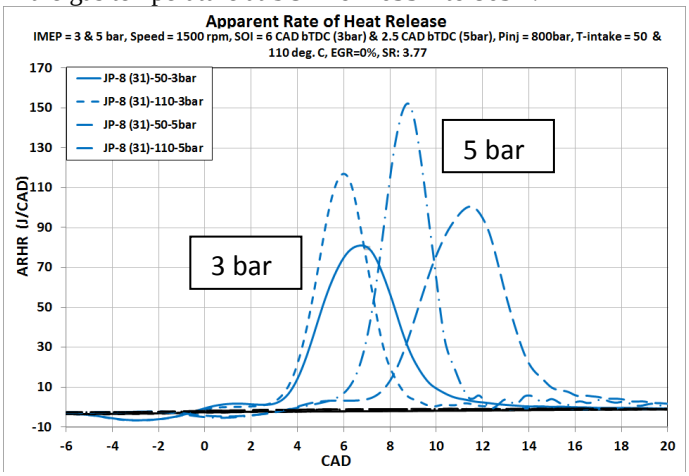

Figure 6: RHR for the JP-8 (31) at two loads and two intake temperatures

Increasing the intake temperature reduced the ignition delay at two loads; however, it increased the pre-mixed combustion fraction at higher load. This implies that the increase rate of evaporation at the higher temperature, retarded injection and higher equivalence at higher load over-compensated the reduction in the ignition delay period.

The zoomed in RHR traces in Fig. 7 show the effect of the increase in engine load and intake air temperature on LT (Low Temperature) and NTC (Negative Temperature Coefficient) regimes. Both the LT combustion and NTC regimes are observed at the two loads at 50°C intake air temperature. But the drop in RHR in NTC regime is more severe at the lighter load. Increasing intake air temperature to 110°C eliminated NTC regime at IMEP = 3 bar, but kept the LT combustion regime. At IMEP = 5 bar, the increase in temperature eliminated both the LT and NTC regimes.

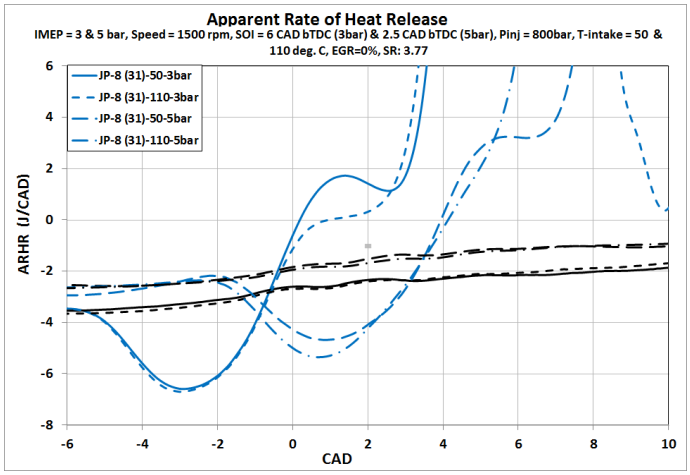

Figure 7: Details of RHR during auto-ignition and early stages of combustion for JP-8 (31) at two loads and two intake temperatures

The ID for JP-8 (31) at the two loads and intake temperatures is plotted versus the mean temperature during ignition delay. The points that exhibited the two-stage auto-ignition are circled. At 3 bar IMEP, all the points, except the highest temperature exhibited NTC, whereas at 5 bar the NTC regime occurred only at low mean temperatures.

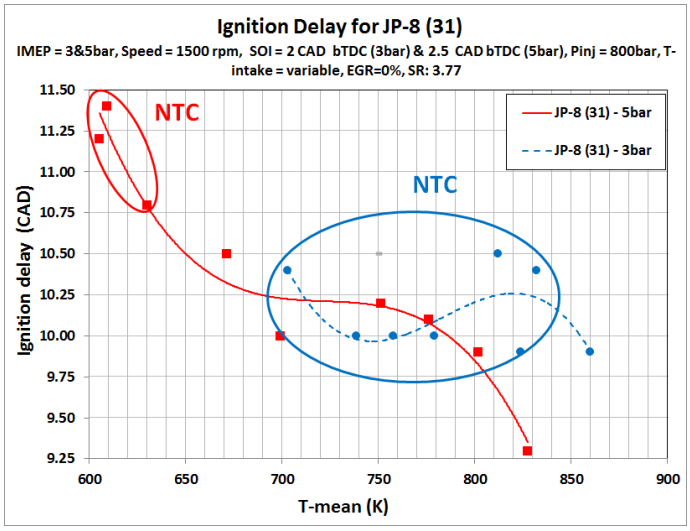

Figure 8: Ignition delay for JP-8 (31) at both loads

Figure 8 shows a drop in the mean pressure during ID at higher mean temperatures. NTC regime occurs in two zones; 'high pressure – low temperature' zone and 'low pressure – high temperature' zone. Previous investigation reported higher mean temperatures and pressures reduce NTC regime [12]. At 3 bar IMEP, all the points exhibited NTC because of lower pressures except at 860K mean temperature. At 5 bar load, points with mean temperatures below 650K exhibited NTC regime. At 3 bar IMEP, the NTC is predominantly controlled by the mean pressure whereas at 5 bar IMEP, NTC was predominantly controlled by mean temperature.

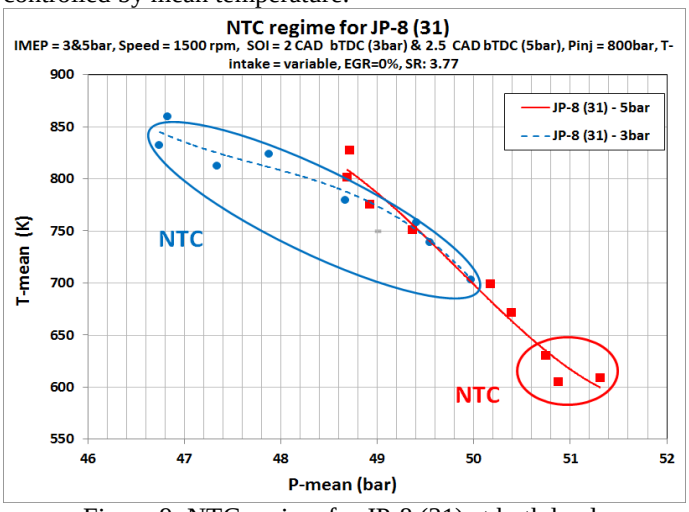

Figure 9: NTC regime for JP-8 (31) at both loads

Increase in mean pressure and equivalence ratio reduced the tendency of NTC behavior [13]. At 5 bar IMEP, this effect is observed.

Effect of intake air temperature and fuel properties on Combustion

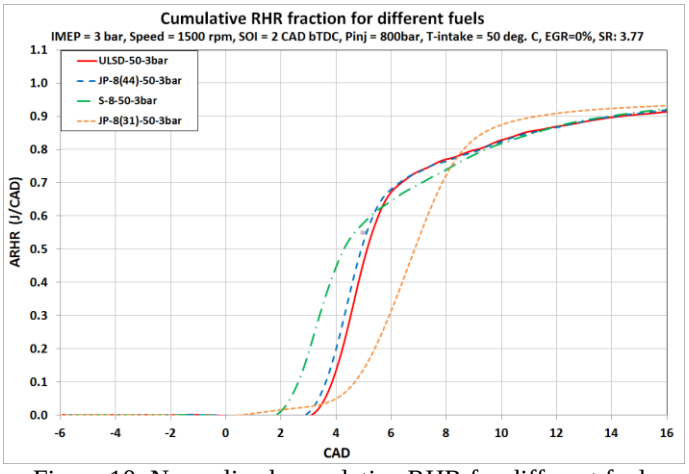

Figure 10: Normalized cumulative RHR for different fuels

To compare between the mass fractions of the fuel burned at different stages of combustion, the normalized integral of the RHR is calculated from the start of injection to the exhaust valve opening [8, 14, 15] and plotted in Fig. 10. The sharp rise indicates the premixed combustion heat release. Fig. 11a & 11b show the mass fraction of the fuel burned in pre-mixed mode for the four fuels at 3 & 5 bar IMEP at 50°C & 110°C intake temperatures. JP-8 (31) has the highest premixed combustion fraction, mainly because it has the longest ID period that allows more time for fuel evaporation and mixing before auto-ignition. On an average JP-8 (31) combustion was predominantly premixed (around 80% on an average). Tendency for NTC behavior is higher if the mixture is more homogenous [16].

Figure 11 shows also increasing the inlet temperature from 50°C to 110°C reduced the premixed combustion fraction for all the fuels except the JP-8 (31) at IMEP = 5 bar. Raising the gas temperature affects the premixed combustion fraction as it increases the rate of evaporation. But at the same time it accelerates the auto-ignition reactions. The data in Figure 11 indicates clearly that the increase in the reaction rates is faster than the increase in evaporation rate for the three fuels. F-T SPK produced the lowest pre-mixed fraction because of very high cetane number and hence it produced lower peaks of RHR compared to other fuels as shown Fig. 3.

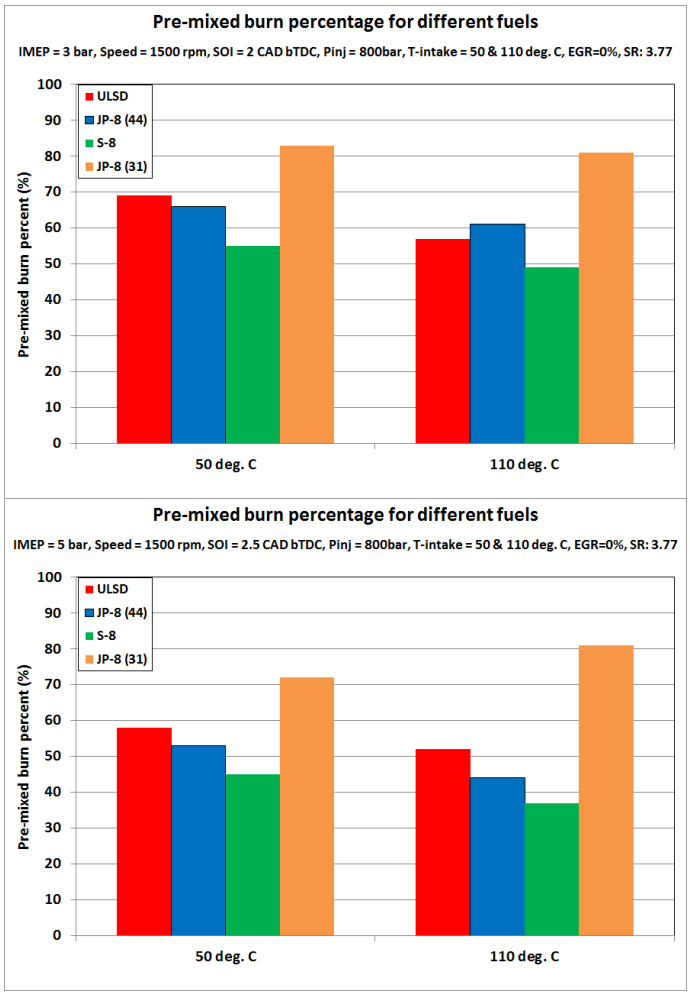

Figure11 a & b: Premixed combustion fraction for different fuels at 3 bar and 5 bar IMEP respectively

Arrhenius plots

Definitions of ignition delay

Ignition delay is the time elapsed between the start of injection and start of combustion. Many criteria have been used to identify the start of combustion. These include that point at which one of the following parameters is reached: a certain percentage of heat release rate [8, 14, 17], a specified pressure rise due to combustion [18, 19, 20] and luminescence [19, 21]. In this investigation the start of combustion is considered to be the point where the dP/dΘ in the firing pressure trace is 'zero' or where dP/dΘ switches from a negative value to a positive value as illustrated in Figure 12.

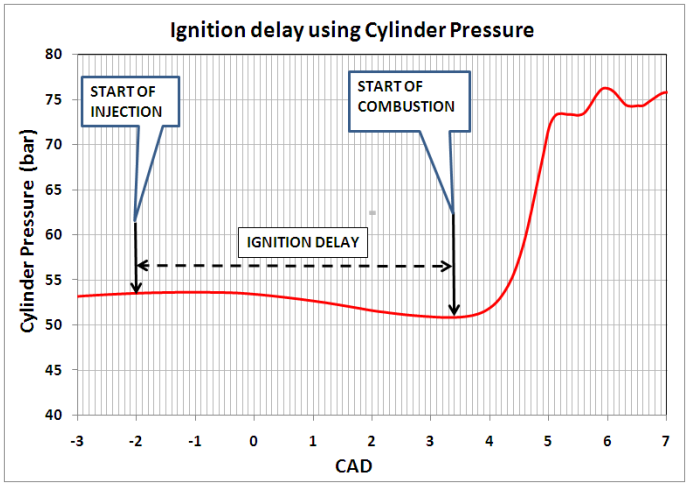

Figure12: Ignition delay definition using pressure trace

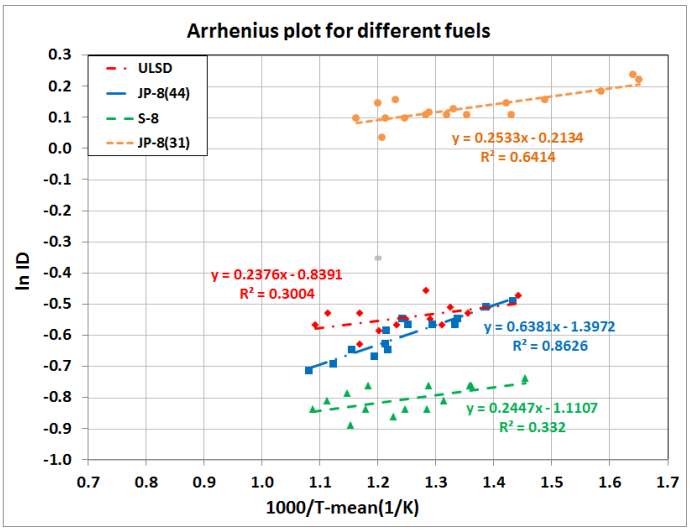

Figure13: Arrhenius plots for different fuels

Arrhenius plots are used to calculate the global activation energy of the auto-ignition reactions for each fuel. Natural logarithm of ignition delay (Y-axis) is plotted against the inverse of the absolute mean temperature during ignition delay (X-axis). The slope of the line of best fit gives the term (E/R) given in equation (1) [22]. Where E is the global activation energy and R is the universal gas constant. T_a is the ambient temperature which is considered to be T-mean during ignition delay. Equations of the trend lines are displayed beside the lines.

$$\tau_{ig} = A\exp(E/RT_a)[O_2]^n \quad \text{-------(1)}$$

Fuel	Activation Energy (J/mol)
ULSD	1975
JP-8 (44)	5305
F-T SPK	2034
JP-8 (31)	2106

(Table 1: Activation energy for different fuels)

It can be observed from the table 1 above that JP-8 (44) has the maximum activation energy probably because of low cetane number. A similar effect was observed with F-T SPK as it produced low activation energy as it has a very high cetane number (>74). But this effect was not observed with JP-8 (31) which was expected to produce the maximum activation energy. It can be observed that activation energy cannot be related only to the cetane number of the fuel.

CONCLUSIONS

The following conclusions are based on an experimental investigation on a single-cylinder research direct injection diesel engine equipped with a common rail injection system. Shop air is used to supercharge the engine and an electric heater is used to control the intake air temperature. Four fuels of different cetane Numbers, varying from 31 to 74 are tested at two loads: IMEP = 3 and 5 bar and temperatures varying from 50°C to 110°C. The fuel with the lowest CN experienced both the LT and NTC combustion regimes. A CFD code coupled with heptane combustion mechanism is applied, using the geometry and operating conditions of the engine. The model produced the mole fraction of 33 intermediate species from the SOI to the exhaust valve opening. A detailed analysis of the simulation model and the experimental data resulted in the following conclusions:

1. The lowest CN fuel, JP-8 (31) experienced the two-stage auto-ignition: the low temperature combustion (LT) and negative temperature coefficient (NTC) regimes under the two loads.
2. LT and LTC regimes are prominent at the low load under all temperature except the highest. At the highest intake temperature NTC regime disappears, but LT regime is sustained. At the higher load LT and NTC regimes appear, only at the low intake temperatures.
3. The simulation model showed clearly that NTC regime is associated with the presence of high mole fractions of formaldehyde. As HCHO starts to disappear, the oxidation reactions increase at a sharp rate.

4. The model results agree with the experimental data on the effect of the increase in the gas temperature in changing the extent of the LT and NTC regimes.
5. The premixed combustion fraction of a fuel is closely but inversely related to its CN. High CN fuels burn less in the premixed combustion mode.
6. The global activation energy for the auto-ignition reactions is calculated for the four fuels and was found out that global activation energy cannot be related to cetane number of fuel alone.

ACKNOWLEDGMENTS

This research was sponsored by US Army TARDEC, NAC, US Department of Energy, Next Energy and Automotive Research Center (ARC): A Center of Excellence in Simulation and Modeling sponsored by US Army TARDEC and directed by University of Michigan. Our special thanks are to Laura Hoogterp and Eric Sattler of US Army TARDEC and NAC. We would like to thank Rolando Moya Ferrer for his help in the engine tests, NBEL team, Lidia Nedeltcheva and Eugene Snowden and WSU CAR members.

REFERENCES

1. Siebers, D. L., "Ignition Delay Characteristics of Alternative Diesel Fuels: Implication on Cetane Number", SAE 852102.
2. Pickett, L., Hoogterp, L., "Fundamental spray and combustion measurements of JP-8 at diesel conditions", SAE 2008-01-1083
3. Frame, E. A. et. al., "Alternative Fuels: Assessment of Fischer-Tropsch Fuel for Military Use in 6.5L Diesel Engine", SAE 2004-01-2961
4. Schihl, P., et. al., "Assessment of JP-8 and DF-2 Evaporation Rate and Cetane Number Differences on a Military Diesel Engine", SAE 2006-01-1549
5. Papagiannakis, R.G. et. al., "Single Fuel Research Program Comparative Results of the Use of JP-8 Aviation Fuel versus Diesel Fuel on a Direct Injection and Indirect Injection Diesel Engine", SAE 2006-01-1673
6. Lepperhoff, G., et. al., "Potential of Synthetic Fuels in Future Combustion Systems for HSDI Diesel Engines", SAE2006-01-0232
7. Flynn, P. F., et. al., "Diesel combustion: An integrated view combining laser diagnostics, chemical kinetics, and empirical validation", SAE 1999-01-0509
8. Nargunde, J., Jayakumar, C., et. al., "Comparison between Combustion, Performance and Emission Characteristics of JP-8 and Ultra Low Sulfur Diesel Fuel in a Single Cylinder Diesel Engine", SAE 2010-01-1123
9. Bekdemir, C., et. Al., "On the application of the Flamelet Generated Manifold (FGM) Approach to the simulation of an Igniting Diesel Spray", SAE 2010-01-0358.
10. Jansons, M., et. al., "Experimental Investigation of Single and Two-Stage Ignition in a Diesel Engine", SAE 2008-01-1071
11. V. Nagaraju, N. Henein, A. Quader, M. Wu, W. Bryzik, "Effect of Biodiesel (B-20) on Performance and Emissions in a Single Cylinder HSDI Diesel Engine", SAE 2008-01-1401, 2008
12. Pfahl, U., "Self-ignition of diesel-engine model fuels at high pressures" SAE 1997 – 970897
13. Minagawa, T., et. al., "A study on ignition delay of diesel fuel spray via numerical simulation", SAE 2000-01-1892
14. Jayakumar, C., Nargunde, J., et. Al., "Effect of Biodiesel, JP-8 and Ultra Low Sulfur Diesel Fuel on Auto-ignition, Combustion, Performance and Emissions in a Single Cylinder Diesel Engine", ASME ICEF 2010-35060
15. Miles, P. C., "The Influence of Swirl on HSDI Diesel Combustion at Moderate Speed and Load", SAE 2000-01-1829
16. Ishiyama, T.,et. al., "Modeling and Experiments on Ignition of Fuel Sprays Considering the Interaction Between Fuel-Air Mixing and Chemical Reactions", SAE 2003-01-1071
17. Lin, C. S. and Foster, D. E.," An Analysis of Ignition Delay, Heat Transfer and Combustion During Dynamic Load Changes in a Diesel Engine," SAE 892054, 1989
18. Hoskin, D. H., Edwards, C.F. and Siebers, D. L., "Ignition Delay Performance vs. Composition of Model Fuels", SAE 920109, 1992
19. Edwards, C. F., Siebers, D. L. and Hoskin, D. H.,"A Study of the Autoignition Process of a Diesel Spray via High Speed Visualization" SAE 920108, 1992
20. Aligrot, C., Champoussin, Guerrassi, N. and Claus, G., A Correlative Model to Predict Autoignition Delay of Diesel Fuels," SAE 970638, 1997
21. Kwon, S., Arai, M, and Hiroyasu, H.,"Ignition Delay of a Diesel Spray Injected into Residual Gas Mixture," SAE 911841
22. Pickett, L. M., et. al., "Relationship Between Ignition Processes and the Lift-Off Length of Diesel Fuel Jets", SAE 2005-01-3843

ACRONYMS AND ABBREVIATIONS

- A – Pre-exponential factor used in [19])
- ARHR – Apparent Rate of Heat Release
- aTDC– After Top Dead Center
- bTDC– Before Top Dead Center
- CAD – Crank Angle Degree
- CN –Cetane number
- C.R. – Compression ratio
- E – Activation energy
- ECM – Engine Control Module
- EGR – Exhaust Gas Recirculation

- EVO – Exhaust valve opening
- F-T SPK – Fischer-Tropsch Synthetic Paraffinic Kerosene
- HSDI – High Speed Direct Injection
- HV – Heating Value
- ID – Ignition Delay
- IMEP – Indicated Mean Effective Pressure
- LT – Low temperature
- n – Empirical constant (used in [19])
- NTC – Negative Temperature Coefficient
- R – Universal gas constant
- RHR – Rate of Heat Release (same as ARHR)
- SOI – Start of Injection
- TDC – Top Dead Center
- T_a – Ambient temperature (used in [19])
- τ_{ig} – Ignition delay (used in [19])
- ULSD – Ultra Low sulfur diesel

APPENDIX A

EXPERIMENTAL CONDITIONS AND TEST MATRIX

TEST MATRIX AND EXPERIMENTAL CONDITIONS		
FUELS	ULSD, JP-8 (CN#44), F-T SPK, JP-8(CN#31)	ULSD, JP-8 (CN#44), F-T SPK, JP-8(CN#31)
INJECTION PRESSURE (in Bars)	800	800
ENGINE SPEED (rpm)	1500	1500
LOAD	**3 bar IMEP**	**5 bar IMEP**
SWIRL	3.77	3.77
EGR	0%	0%
START OF INJECTION	**-2.0 CAD* bTDC**	**-2.5 CAD bTDC**
INJECTION DURATION	**0.358 ms**	**0.402 ms**
INTAKE AIR PRESSURE	1.1 bar	1.1 bar
INTAKE AIR TEMPERATURE	30^0C-110^0C	30^0C-110^0C
EXHAUST GAS PRESURE	1.1 bar	1.1 bar
COOLANT OUTLET TEMPERATURE	82.2^0C	82.2^0C

*JP-8 (31) was injected at -6.0 CAD for 3 bar IMEP tests as it misfired at -2.0 CAD

APPENDIX B

FUEL PROPERTIES

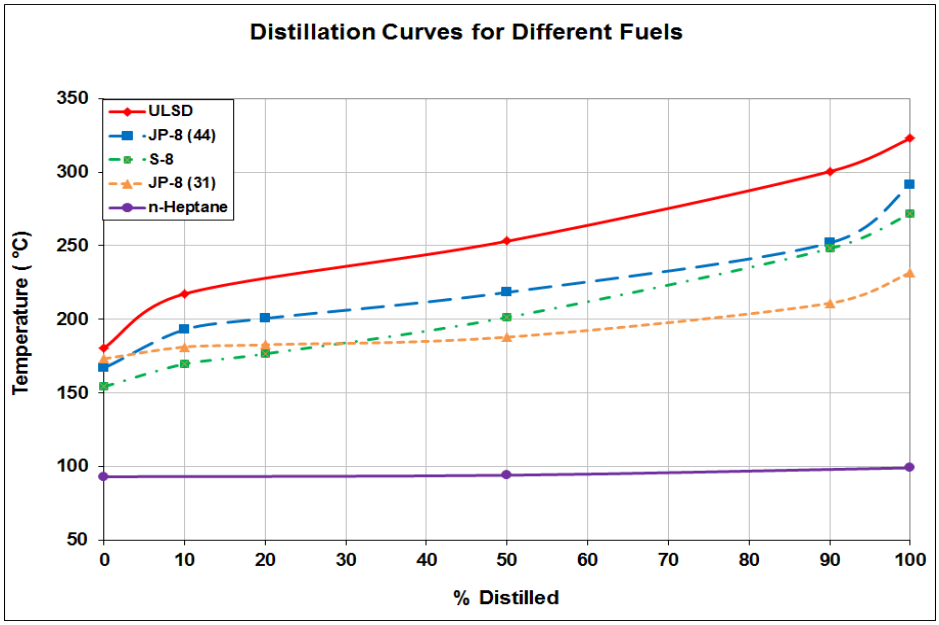

Property	ULSD	JP-8 (44)	F-T SPK	JP-8 (31)	Heptane
Flash point (^{0}C)	64	56.8	37.8	53	-4
Density (Kg/m3)	836.5	770	736.2	768.8	669
Cetane Number	45.3	44.1	>74	31	56
Lower Heating Value (MJ/Kg)	41.2	42.1	44.1	44.0	44.6

APPENDIX C

Arrhenius coefficients for some reactions consuming OH radical in the earlier stages of combustion

Reactions	Arrhenius coefficients					
	Forward Reaction			Backward reaction		
	A	n	Ea (KJ/mol)	A	n	Ea (KJ/mol)
NC7H16+OH=C7H15-2+H2O	***4.5E9***	***1.3***	***4.56***	***2.997E5***	***2.19***	***88.86***
CO+OH=CO2+H	8.98E7	1.38	21.89	2.64E14	0.177	130.25
H2+OH=H2O+H	1.17E9	1.3	15.17	1.25E10	1.19	79.32
CH2O+OH=HCO+H2O	5.6E10	1.1	-0.32	1.09E9	1.43	119.24
CH4+OH=CH3+H2O	1.6E6	2.1	10.29	5.8E4	2.28	68.44